

## **Supporting information for**

# **Engineering of Bi-S<sub>3</sub> and Sulfur-Vacancy Dual Sites for Efficient Photocatalytic N-alkylation of amines**

Gang Wang,<sup>#a</sup> Yan Liu,<sup>#a</sup> Jiangwei Zhang,<sup>#b</sup> Qingqing Chen,<sup>a</sup> Kai Fang,<sup>a</sup> Junjie Mao<sup>\*a</sup>

<sup>a</sup>. Key Laboratory of Functional Molecular Solids, Ministry of Education, College of Chemistry and Materials Science, Anhui Normal University, Wuhu 241002, P. R. China.

<sup>b</sup>. Dalian Institute of Chemical Physics, Chinese Academy of Sciences, Dalian 116023, P. R. China.

<sup>#</sup> These authors contributed equally to this work.

<sup>\*</sup> E-mail: maochem@ahnu.edu.cn

## Supporting Materials and Methods

### Materials

Zinc nitrate hexahydrate ( $\text{Zn}(\text{NO}_3)_2 \cdot 6\text{H}_2\text{O}$ ), Zinc acetate dihydrate ( $\text{Zn}(\text{CH}_3\text{COO})_2 \cdot 2\text{H}_2\text{O}$ ), L-Cysteine, Indium nitrate hydrate ( $\text{In}(\text{NO}_3)_3 \cdot x\text{H}_2\text{O}$ ), Thioacetamide (TAA), hydrochloric acid (HCl), Bismuth (III) nitrate pentahydrate ( $\text{Bi}(\text{NO}_3)_3 \cdot 5\text{H}_2\text{O}$ ), Bismuth trichloride ( $\text{BiCl}_3$ ) Polyvinylpyrrolidone (PVP, K-30),  $\text{NaBH}_4$ , Potassium tert-butoxide (t-BuOK), Triethanolamine (TEOA), Aniline, Benzyl alcohol, ethanol, ultra-dry acetonitrile, N, N-Dimethylformamide (DMF) were purchased from Alfa Aesar company. Nafion 117 solution was purchased from DuPont. 18.2  $\text{M}\Omega \cdot \text{cm}$  ultrapure water was purified by milli-Q instrument. All the chemicals were analytical grade and used without further purification.

### Preparation of S-V<sub>s</sub>

2.50 mmol  $\text{Zn}(\text{NO}_3)_2 \cdot 6\text{H}_2\text{O}$ , 5.00 mmol  $\text{In}(\text{NO}_3)_3 \cdot x\text{H}_2\text{O}$  and 0.01 mol TAA were mixed together into 60 mL ultrapure water. The pH value of the solution was adjusted to about 1.00 by the hydrochloric acid solution after fully dissolved under constant stirring. After that, the transparent solution was transferred to a 100 mL sealed Teflon-lined autoclave and heated at 433 K for 12 h. The yellow suspension was washed with water and ethanol for several times after the autoclave slowly cooled down to room temperature. Finally, the obtained sample was dried at 333 K overnight.

### Preparation of Bi-S<sub>3</sub>/S-V<sub>s</sub>

0.50 g as-obtained S-V<sub>s</sub> was dispersed into 40.0 mL ultra-dry acetonitrile and 5.0 mL TEOA mixed solution under constant stirring. Then, 0.012 g  $\text{Bi}(\text{NO}_3)_3 \cdot 5\text{H}_2\text{O}$  was

added into above suspension. Bi single atoms were successfully loaded on S-V<sub>s</sub> nanosheets after 5 min light irradiation. The dark yellow sample was obtained after washing with water and ethanol several times, and then dried in a vacuum overnight at 333 K.

#### **Preparation of Bi NPs/S-V<sub>s</sub>**

Bi nanoparticles (Bi NPs) were synthesized according to the previous report.<sup>1</sup> 0.316 g of BiCl<sub>3</sub> and 1.116 g PVP was added into 37.92 g DMF solution under magnetic stirring. After dissolution, 0.116 g NaBH<sub>4</sub> was added into the solution to reduce the Bi<sup>3+</sup>. The dark solution was stirred and alternatively ultrasonic dispersion for 45 min. The Bi NPs were thoroughly washed (four times) and storage with acetone. Bi NPs/S-V<sub>s</sub> was obtained via mixing Bi NPs (0.89 wt %) with S-V<sub>s</sub> powder together.

#### **Preparation of ZnIn<sub>2</sub>S<sub>4</sub> hierarchical microspheres without S vacancies (ZIS)**

ZIS was synthesized via the previously reported method with a slight modification.<sup>2</sup> 0.5 mmol of Zn(CH<sub>3</sub>COO)<sub>2</sub>•2H<sub>2</sub>O, 1 mmol of In(NO<sub>3</sub>)<sub>3</sub>•xH<sub>2</sub>O and 8 mmol of L-Cysteine were dissolved in 80 mL of deionized water. After that, the solution was transferred into a 100 mL sealed Teflon-lined autoclave and heated at 453 K for 12 h. The yellow suspension was washed with water and ethanol for several times after the autoclave slowly cooled down to room temperature. Finally, the obtained sample was dried at 333 K overnight.

#### **Characterizations**

The microstructure and morphologies of the photocatalysts were analyzed by transmission electron microscopy (TEM, JEOL 200CX), high-resolution transmission electron microscopy (HRTEM, JEM-2010F) with an energy-dispersive X-ray (EDX)

spectrometer, and scanning electron microscopy (SEM, Hitachi S-4800). Crystal phase identification was conducted via a powder X-ray diffraction (XRD, D/MAX-2550) using Cu K $\alpha$  radiation. X-ray photoelectron spectroscopy (XPS) tests were performed on a PHI ESCA-5000C electron spectrometer. The Raman spectra were analyzed by a Renishaw in Via Raman spectrometer. UV/vis diffuse reflectance spectra (DRS) of the photocatalysts were recorded on a Hitachi U-3010 spectrophotometer. Fourier transform infrared (FT-IR) spectra (4000-400 cm<sup>-1</sup>) were obtained from KBr pellets using a Bruker Tensor 22 instrument. The concentrations of elements were measured with a Thermo Scientific Plasma Quad inductively coupled plasma atomic emission spectroscopy (ICP-AES). *In-situ* FTIR spectra measurements were performed using a Bruker INVENIO R Fourier-transform spectrometer. Photoluminescence (PL) properties and time-resolved photoluminescence (TRPL) spectra of samples were measured on fs980 and Horiba Fluomax-4, respectively. The average blue LED light intensity was about 0.53 mW/cm<sup>2</sup>, which was measured by an optical power meter (PL-MW2000).

### ***In-situ* EPR measurements**

*In-situ* EPR measurements were carried out at 77 K using a Bruker A300 spectrometer operating in the X-band (9.64 GHz) and 100 kHz magnetic field modulation (modulation amplitude, 10 G). Liquid nitrogen was used to control the temperature. As for the *in-situ* EPR measurements, Bi-S<sub>3</sub>/S-V<sub>s</sub> powder was dispersed into methanol solution (5 mg mL<sup>-1</sup>). Methanol solution dispersions were examined in sealed quartz tubes after Ar bubbling for the “before photoactivation sample”. Light



was irradiated onto the sealed quartz tube with a Xe lamp for 30 min for the “after photoactivation sample”. For “after regeneration sample”, O<sub>2</sub> gas was purged to the “after photoactivation sample” for 30 min. All quartz tubes were frozen and stored at 77 K using liquid nitrogen before EPR measurements.

### **XAFS measurements and analysis**

The X-ray absorption fine structure of Bi L3-edge was collected at 1W1B beamline of Beijing Synchrotron Radiation Facility (BSRF). The acquired EXAFS data were processed according to the standard procedures using the ATHENA module of Demeter software packages. The EXAFS spectra were obtained by subtracting the post-edge background from the overall absorption and then normalizing with respect to the edge-jump step. Subsequently, the  $\chi(k)$  data of Fourier transformed to real (R) space were obtained by using a hanning windows ( $dk=1.0 \text{ \AA}^{-1}$ ) from different coordination shells to separate the EXAFS contributions. To obtain the quantitative structural parameters around central atoms, least-squares curve parameter fitting was performed via using the ARTEMIS module of Demeter software packages.

The following EXAFS equation was used:

$$\chi(k) = \sum_j \frac{N_j S_o^2 F_j(k)}{k R_j^2} \exp[-2 k^2 \sigma_j^2] \exp\left[-\frac{2 R_j}{\lambda(k)}\right] \sin[2k R_j + \phi_j(k)]$$

The theoretical scattering amplitudes, phase shifts and the photoelectron mean free path for all paths calculated.  $S_o^2$  is the amplitude reduction factor,  $F_j(k)$  is the effective curved-wave backscattering amplitude,  $N_j$  is the number of neighbors in the  $j^{\text{th}}$  atomic shell,  $R_j$  is the distance between the X ray absorbing central atom and the atoms in the  $j^{\text{th}}$  atomic shell (backscatterer),  $\lambda$  is the mean free path in  $\text{\AA}$ ,  $\phi_j(k)$  is the phase shift

(including the phase shift for each shell and the total central atom phase shift),  $\sigma_j$  is the Debye-Waller parameter of the  $j^{\text{th}}$  atomic shell (variation of distances around the average  $R_j$ ). The functions  $F_j(k)$ ,  $\lambda$  and  $\phi_j(k)$  were calculated with the ab initio code FEFF9.

### **Photo-electrochemical performance**

The photo-electrochemical measurements were performed in a 0.5 mol L<sup>-1</sup> Na<sub>2</sub>SO<sub>4</sub> electrolyte solution with a three-electrode system. The as-prepared fluorine doped tin oxide glass (FTO glass) modified films, platinum foil (1×1 cm<sup>2</sup>), and Ag/AgCl (Saturated KCl) were used as the working electrode, counter electrode, and reference electrode, respectively. The results collected on an electrochemical station (CHI660E, China) under light illumination, a 100 W blue LED ( $\lambda = 455\text{nm}$ ) was used as light source. 5.0 mg of the as-prepared photocatalysts and 20  $\mu\text{L}$  of 5 wt % Nafion solution dispersed in 1.0 mL water and sonication for one hour before using. Then, 100  $\mu\text{L}$  of the catalyst colloid was spread on the pretreated FTO glass (1.0×1.0 cm<sup>2</sup>), and dried in air at room temperature to form photocatalysts modified FTO glass. Mott-Schottky plots of photocatalysts in N<sub>2</sub> purged 0.5 mol L<sup>-1</sup> Na<sub>2</sub>SO<sub>4</sub> electrolyte solution with the same three-electrode system.

### **Photocatalytic selective N-alkylation of amines by alcohols**

The selective N-alkylation of amines by alcohols was undertaken at room temperature via using a 100 W blue LED ( $\lambda = 455\text{ nm}$ ) as a light source. In brief, 10 mg photocatalyst was dispersed into 0.05 mL aniline, 0.5 mL benzyl alcohol and 50 mg t-BuOK in a sealed vessel under constantly stirring. Before illumination, the container was kept bubbled with Ar for about 30 min. The distance between the light source and

vessel was set about 10 cm. After 12 h irradiation, the suspension was filtered by porous membrane and the filtrate was monitored by the Thermo Scientific Trace 1300 Gas Chromatograph equip with ISQ 7000 single quadrupole mass spectrometer (GC-MS). In the cycling tests, the products were monitored by GC-MS detector after 12 h light irradiation for every cycling test.

#### **Method for obtained the conversion rate and selectivity**

$$\text{Conversion rate (\%)} = [(C_0 - C_r)/C_0] * 100\%$$

$$\text{Selectivity rate (\%)} = [C_p/(C_0 - C_r)] * 100\%$$

$$\text{Yield (\%)} = (C_p/C_0) * 100\%$$

$C_0$ : the original concentration of anilines.

$C_r$ : the concentration of anilines after reaction.

$C_p$ : the concentration of products after reaction.

#### **The *quasi in-situ* XPS measurement of Bi-S<sub>3</sub>/S-V<sub>s</sub> after anaerobic light irradiation**

The *quasi-in-situ* XPS measurement was employed to investigate the valance change of Bi species after anaerobic light irradiation. In detail, a certain amount of Bi-S<sub>3</sub>/S-V<sub>s</sub> dispersed into benzyl alcohol solution. The suspension was bubbling with argon for about 30 min. The sample (after irradiation Bi-S<sub>3</sub>/S-V<sub>s</sub>) was collected after 2h anaerobic irradiation (blue LED light), and then dried at room temperature in a vacuum. Before test, the after irradiation Bi-S<sub>3</sub>/S-V<sub>s</sub> sample was sealed into the argon atmosphere.

#### **Surface photovoltage spectroscopy (SPS)**

The measurement system of surface photovoltage spectroscopy (SPS) was home-

made. The monochromatic light resource was produced by a 500 W Xe lamp (CHF XQ500W) in conjunction with a double-prism monochromator (Omni- $\lambda$  3005) and the slit width was 3 mm. The samples were measured without further treatment and keep the contact between the sample and the indium tin oxide (ITO) coated glass electrode (Sigma-Aldrich, d=1.2 mm, resistivity: 8-12  $\Omega\cdot\text{cm}^{-2}$ ) was non-ohmic. The photovoltage signal was amplified by a lock-in amplifier (SR830-DSP) with a light chopper (SR540). The resolution of spectrum was 1 nm.

### **Kubelka-Munk theory and Mott–Schottky measurement**

To confirm the bandgap of Bi-S<sub>3</sub>/S-V<sub>s</sub>, Bi NPs/S-V<sub>s</sub> and S-V<sub>s</sub>, the equation is shown below:

$$\alpha h\nu = A(h\nu - E_g)^{n/2}$$

$\alpha$ ,  $\nu$ ,  $E_g$ ,  $h$  and  $A$  represent absorption coefficient, light frequency, band gap, Planck constant and a constant, respectively, in above equation. “n” is a certain number which determined by the optical transition type of semiconductor. Direct transition type n is 1, while indirect transition type n is 4. S-V<sub>s</sub> is a kind of direct transition type semiconductor, this n is 1.

Mott–Schottky plots were collected under 10 mV amplitude with a frequency of 1000 Hz, 2000 Hz and 3000 Hz. The positive slopes of the Mott–Schottky plots further confirm the n-type conductive properties of Bi-S<sub>3</sub>/S-V<sub>s</sub>, Bi NPs/S-V<sub>s</sub> and S-V<sub>s</sub>. The flat band potential is about 0.10 V below the bottom of the conduction band for n-type semiconductors. Therefore, the conduction bands are -0.96, -1.01 and -1.05 V for Bi-S<sub>3</sub>/S-V<sub>s</sub>, Bi NPs/S-V<sub>s</sub> and S-V<sub>s</sub>, respectively.

## Electrochemical measurements for hydrogen transfer behavior

Hydrogen transfer evidence over S-V<sub>s</sub>, Bi-S<sub>3</sub>/S-V<sub>s</sub> and Bi NPs/S-V<sub>s</sub> were carried out via electrochemical testing: the working electrode was the same as above photocatalysts modified FTO glasses, and the cyclic voltammograms of the as-prepared samples were test in 1.0 M KOH solution as electrolyte (scan rate: 50 mV s<sup>-1</sup>) at room temperature. The potential values, E(RHE), were converted from E(Ag/AgCl) according to the formula  $E(\text{RHE}) = E(\text{Ag/AgCl}) + 0.194 + 0.05916 \times \text{pH}$ . In detail, cyclic voltammetry (CV) curves of catalyst-modified fluorine-doped tin oxide (FTO) electrodes in 1.0 M KOH electrolyte were obtained to evaluate the ability of hydrogen transfer in Figure 5d. For the Bi-S<sub>3</sub>/S-V<sub>s</sub> and Bi NPs/S-V<sub>s</sub> electrodes, the peaks at about -0.03 V (vs. RHE) (H<sub>evo</sub>) are attributed to the evolution of hydrogen. Hydrogen adsorption (H<sub>ads</sub>) and desorption (H<sub>des</sub>) occur in the range of 0.1 to 0.5 V vs. RHE, while the peak observed at about 0.6 V (vs. RHE) is ascribed to hydrogen oxidation (H<sub>oxi</sub>). Hydrogen desorption occurs before hydrogen oxidation, suggesting strong adsorption of hydrogen on the surface of Bi-S<sub>3</sub>/S-V<sub>s</sub>, while the Bi NPs/S-V<sub>s</sub> surface displays only weak hydrogen absorption. Such behavior is not observed in the CV curve of S-V<sub>s</sub> (Figure 5d), indicating that the introduction of Bi species was the critical factor for the excellent hydrogen storage property of Bi-S<sub>3</sub>/S-V<sub>s</sub>.

## Computational details

All the density functional theory (DFT) calculations were performed in the Vienna ab initio simulation package (VASP)<sup>3</sup>. Perdew-Burke-Ernzerhof (PBE)<sup>4</sup> exchange-correlation functional and projector augmented-wave (PAW)<sup>5</sup> potential were employed

to describe electronic exchange-correlation effect and electron-ion interaction, respectively. The energy cutoff of 400 eV was employed for the plane wave expansion. A  $3 \times 4$  single atomic layer  $\text{ZnIn}_2\text{S}_4$  (001) surface slabs with 20 Å vacuum region were constructed. The Brillouin zone was sampled by  $3 \times 2 \times 1$  k-meshs in the Monkhorst-Pack<sup>6</sup> scheme. The van der Waals (vdW) interactions were described by Grimme DFT-D3 scheme.<sup>7</sup> The DFT + U calculations were adopted in this work with the U values are 10.5 for Zn 3d orbit.<sup>8</sup> The force and energy convergence criterion were set to be 0.02 eV/Å and  $10^{-5}$  eV, respectively.

## Section 2: Supporting Figures and Tables

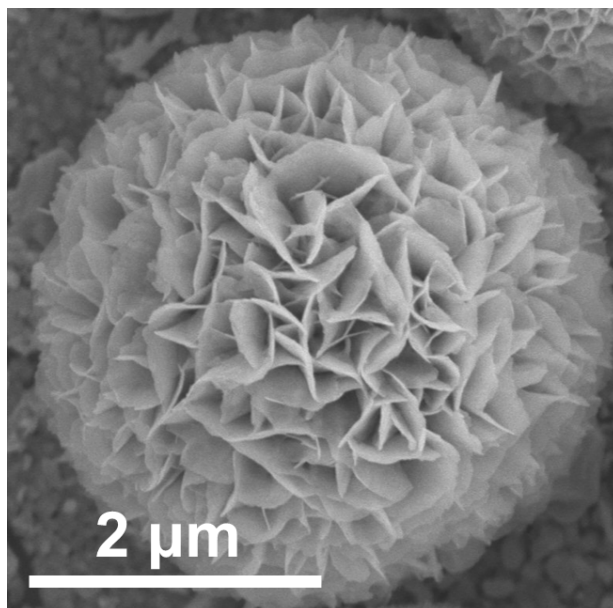


**Figure S1.** SEM image of S-V<sub>s</sub>.

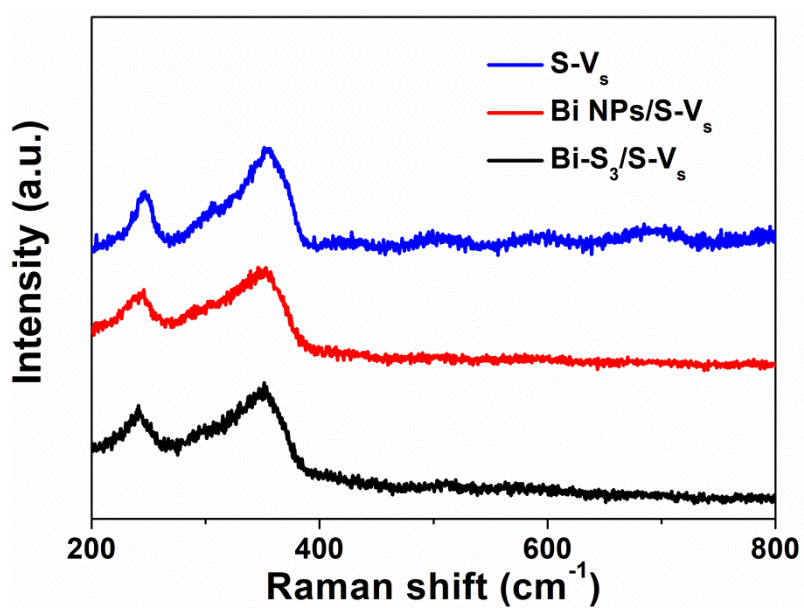


**Figure S2.** Raman spectra of S-V<sub>s</sub>, Bi NPs/S-V<sub>s</sub>, and Bi-S<sub>3</sub>/S-V<sub>s</sub>.

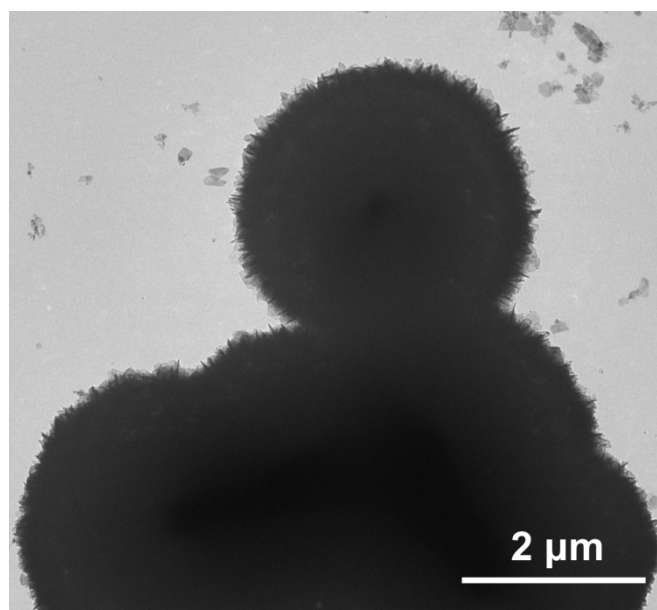


**Figure S3.** TEM image of Bi-S<sub>3</sub>/S-V<sub>s</sub>.

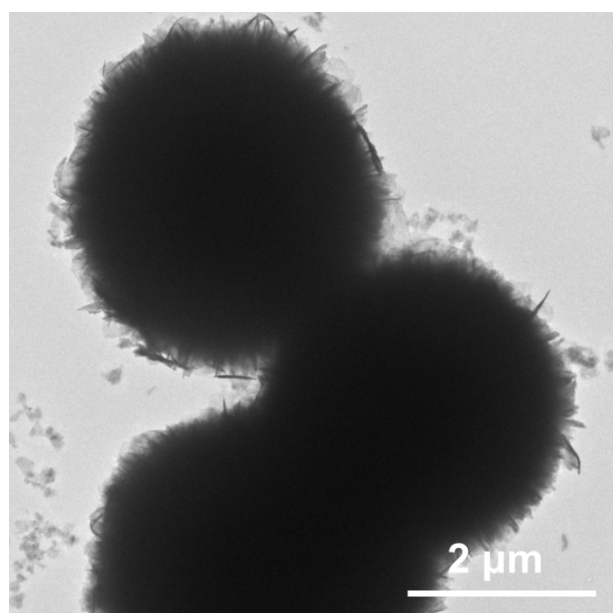


**Figure S4.** TEM image of S-V<sub>s</sub>.



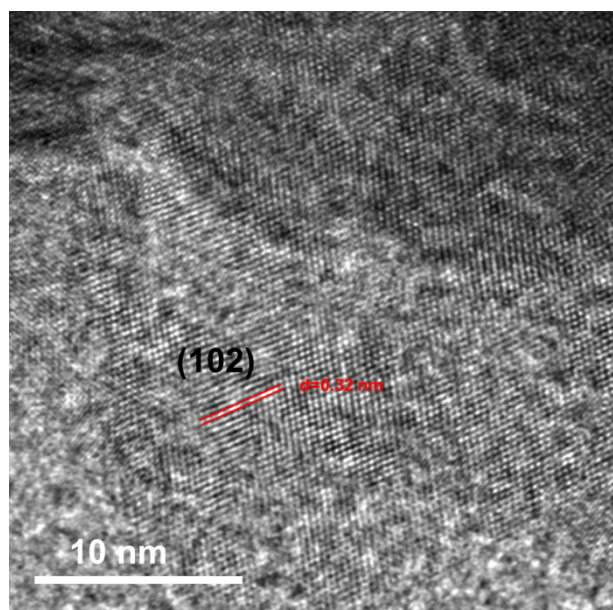


**Figure S5.** The lattice stripe of Bi-S<sub>3</sub>/S-V<sub>s</sub>.

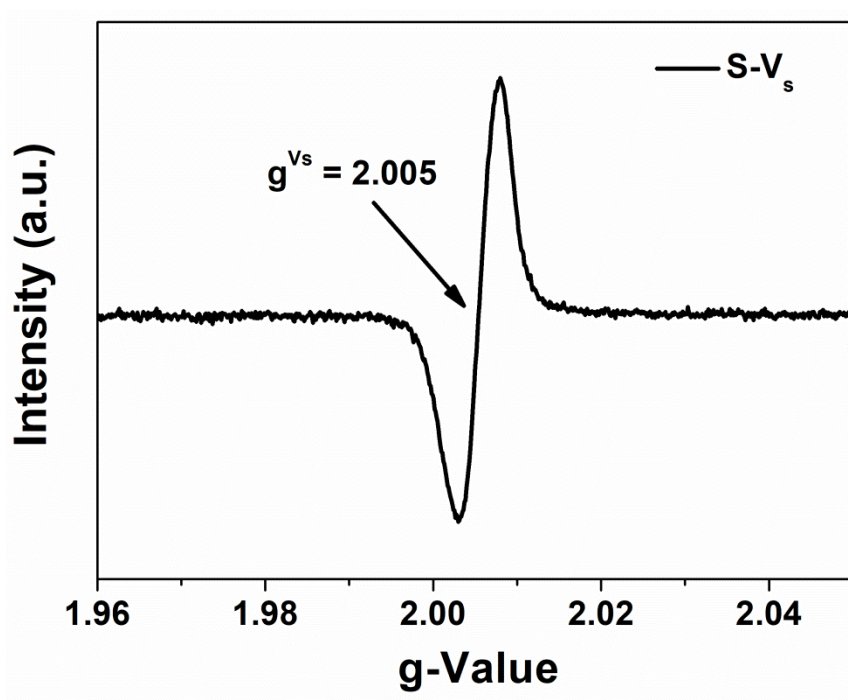


**Figure S6.** EPR g-value of S-V<sub>s</sub>.

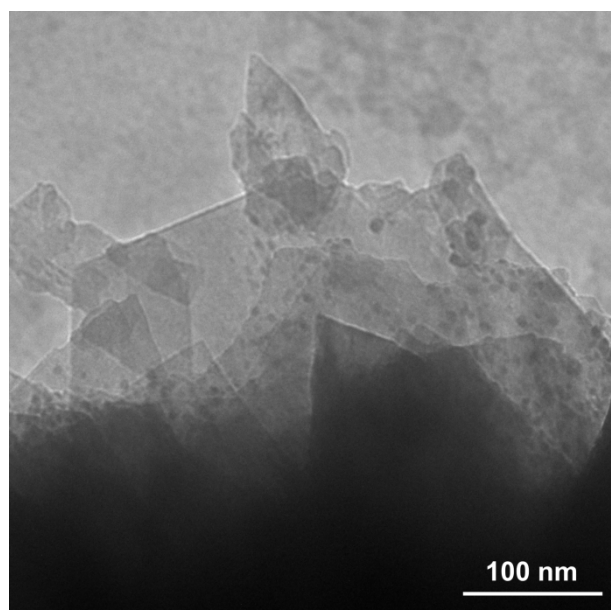


**Figure S7.** TEM image of Bi NPs/S- $V_s$ .

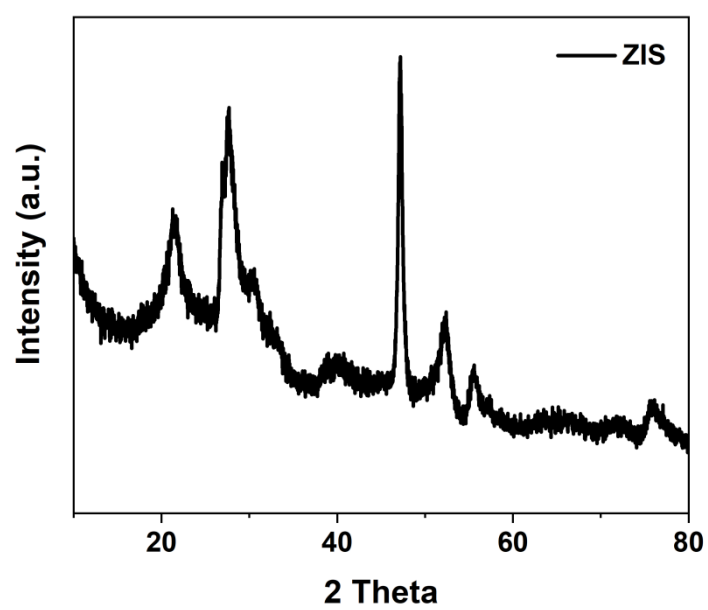


**Figure S8.** XRD pattern of ZIS.

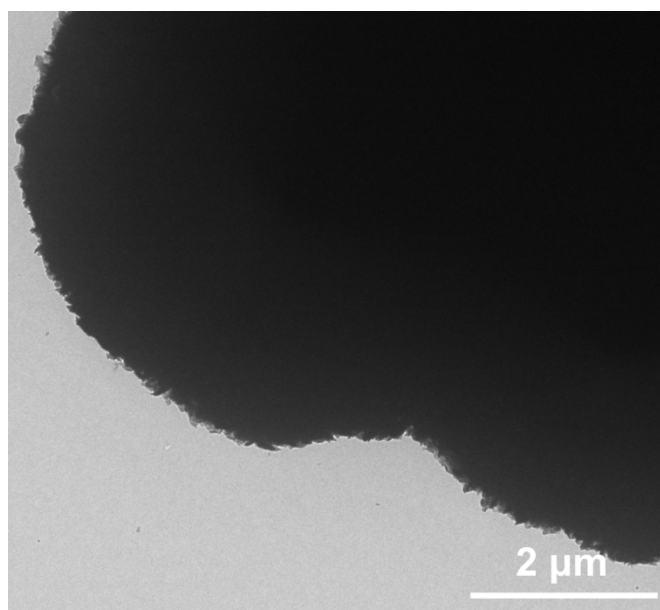


**Figure S9.** TEM image of ZIS.

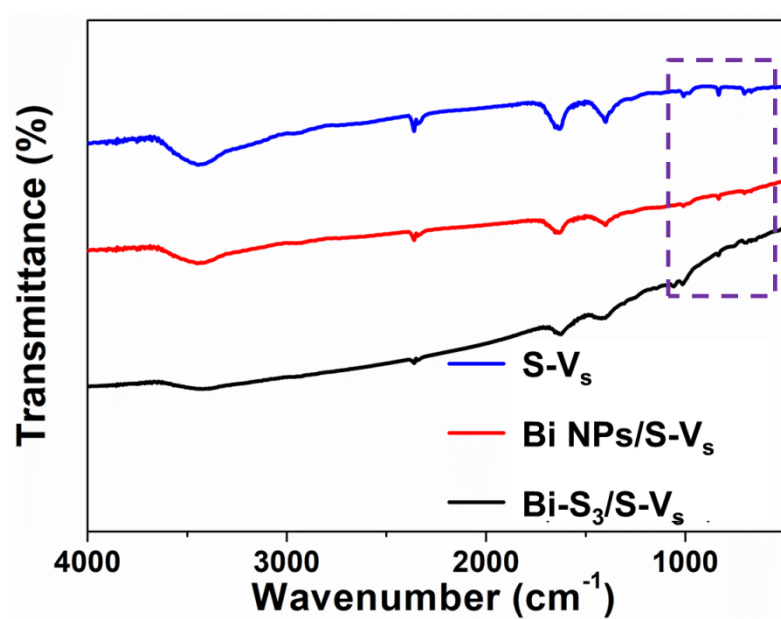


**Figure S10.** FT-IR spectra of samples.

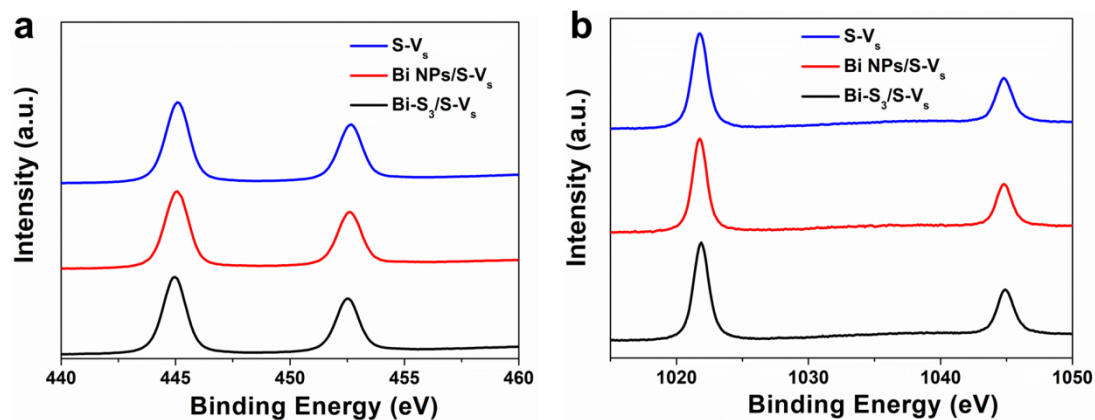


**Figure S11.** XPS spectra of In 3d (a) and Zn 2p (b) over S-V<sub>s</sub>, Bi NPs/S-V<sub>s</sub> and Bi-S<sub>3</sub>/S-V<sub>s</sub>.

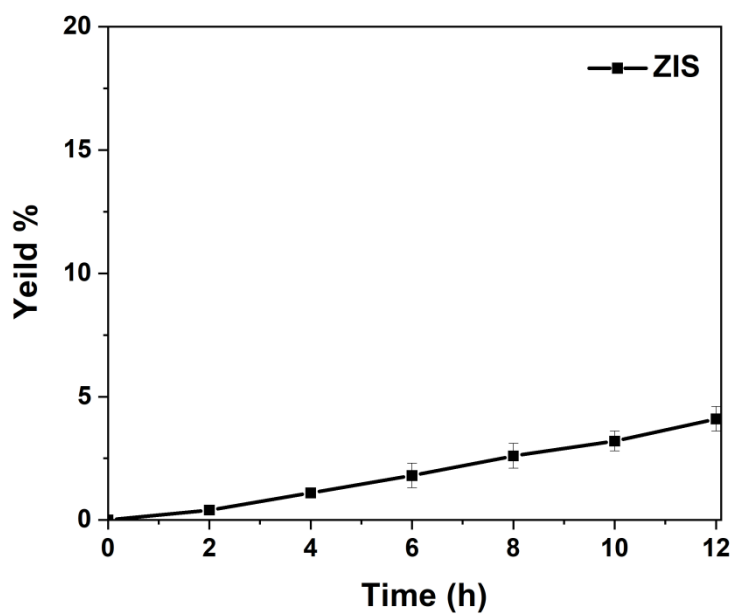


**Figure S12.** Photocatalytic performances for N-alkylation of aniline by benzyl alcohol upon ZIS.

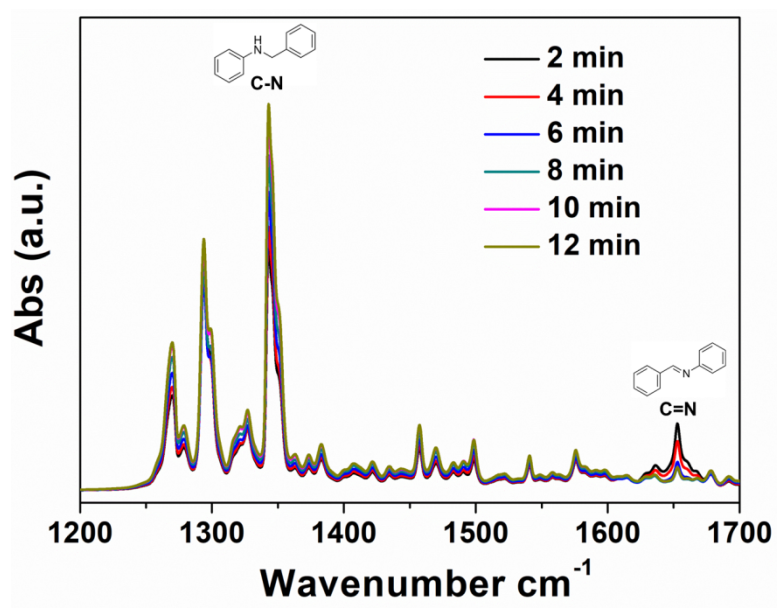


**Figure S13.** *In-situ* FTIR spectra for the N-alkylation of amines reduction process on the Bi-S<sub>3</sub>/S-V<sub>s</sub>.

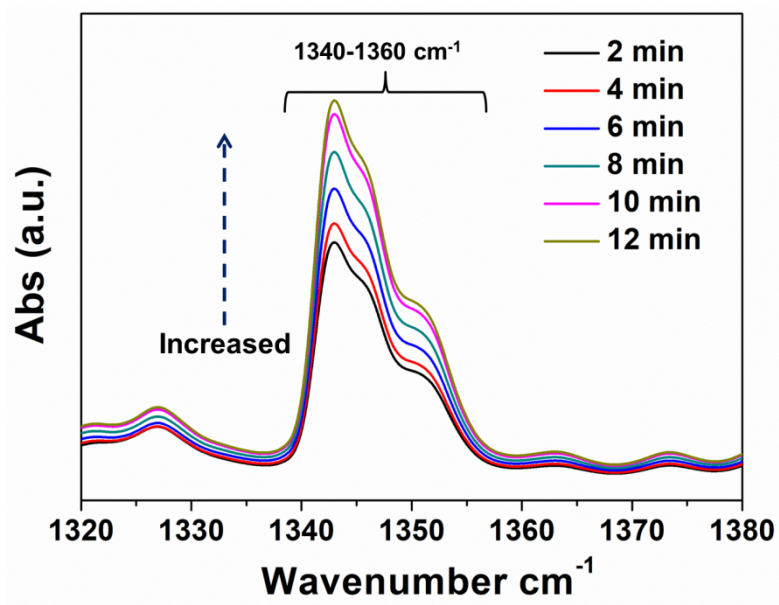


**Figure S14.** *In-situ* FTIR spectra of C-N bond of N-benzylaniline during the photocatalytic reaction.

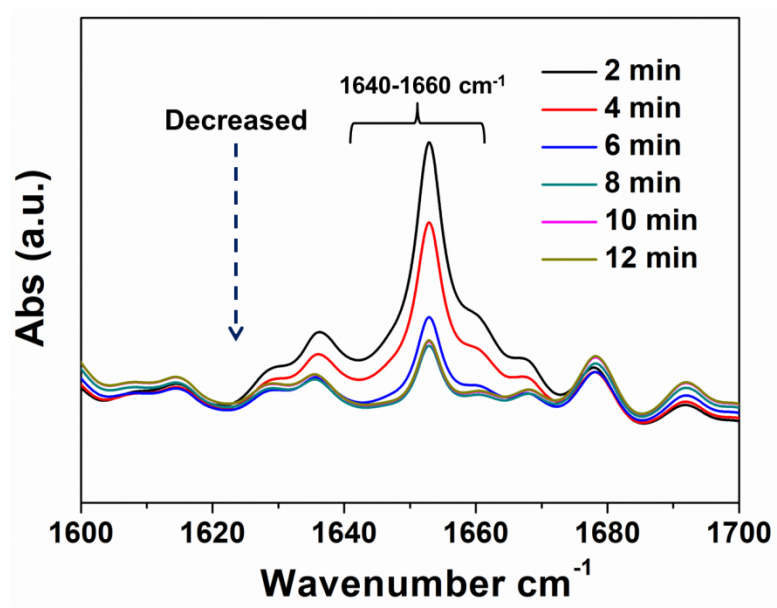


**Figure S15.** *In-situ* FTIR spectra of C=N bond of N-benzylideneaniline during the photocatalytic reaction.

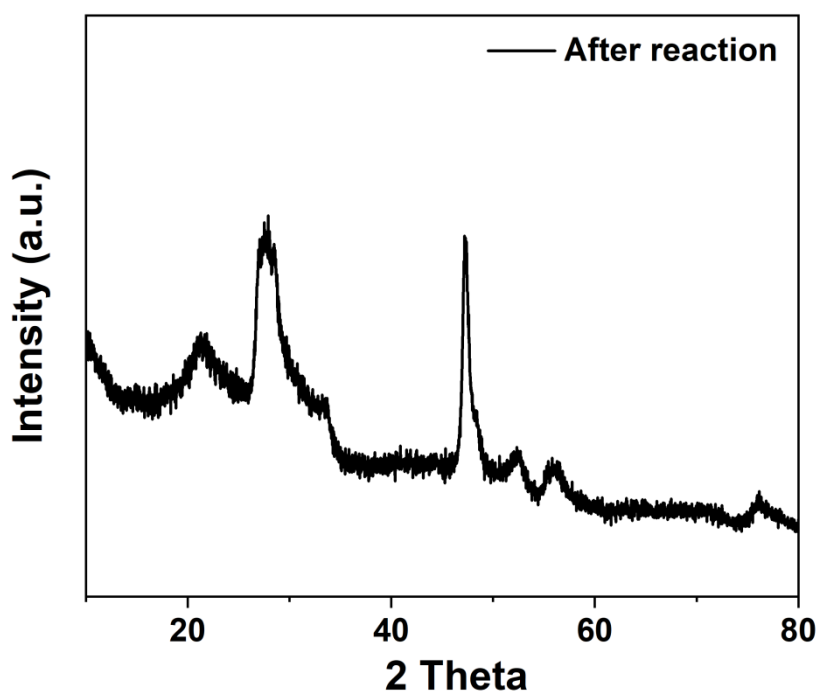


**Figure S16.** XRD pattern of the used Bi-S<sub>3</sub>/S-V<sub>s</sub>.



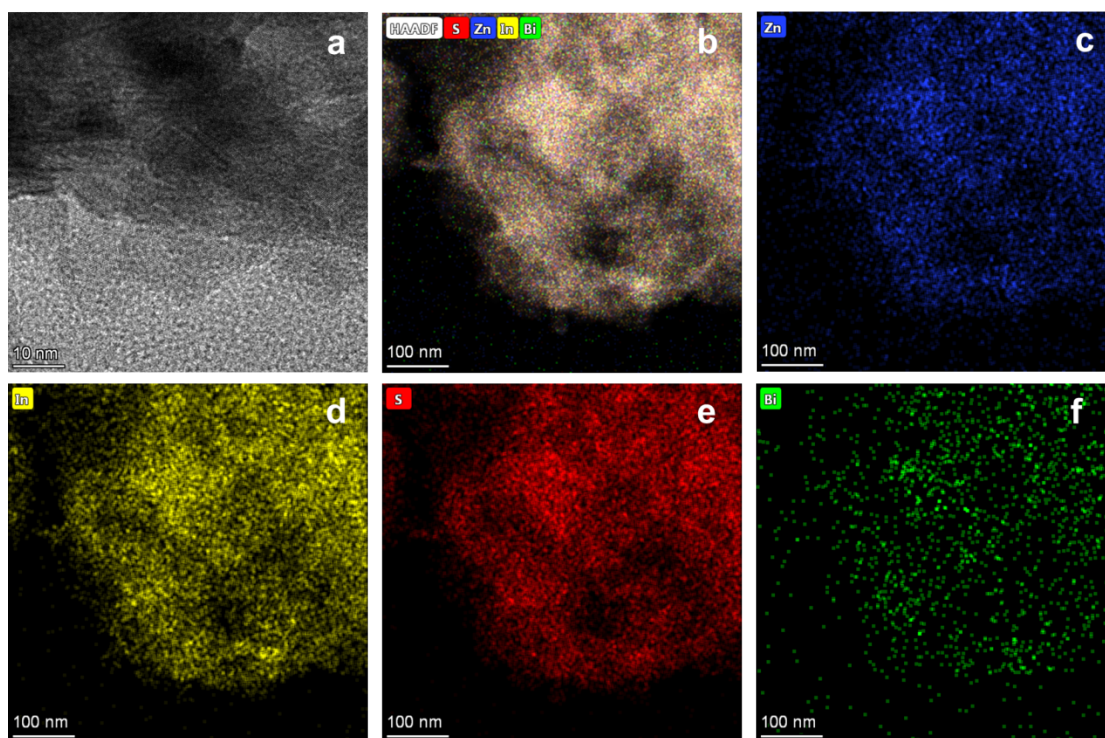


**Figure S17.** (a) TEM image of the used Bi-S<sub>3</sub>/S-V<sub>s</sub>. (b-f) The element mapping results of the used Bi-S<sub>3</sub>/S-V<sub>s</sub>.

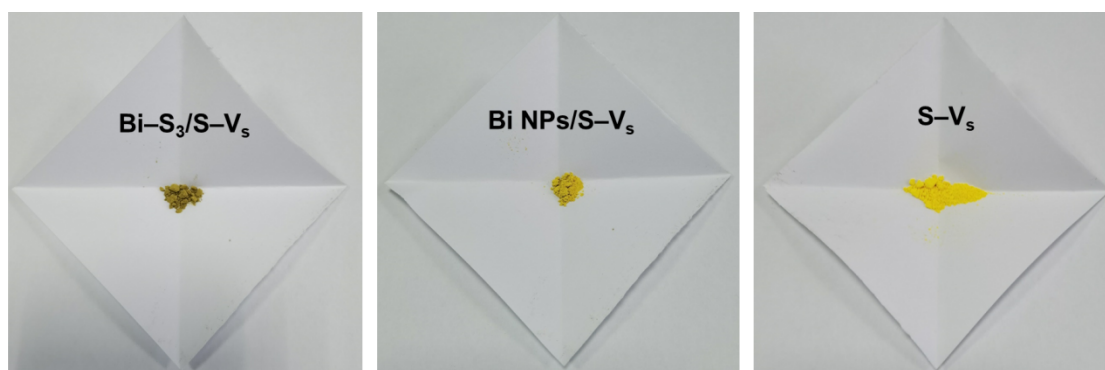


**Figure S18.** The colors of Bi-S<sub>3</sub>/S-V<sub>s</sub>, Bi NPs/S-V<sub>s</sub> and S-V<sub>s</sub> photocatalysts.

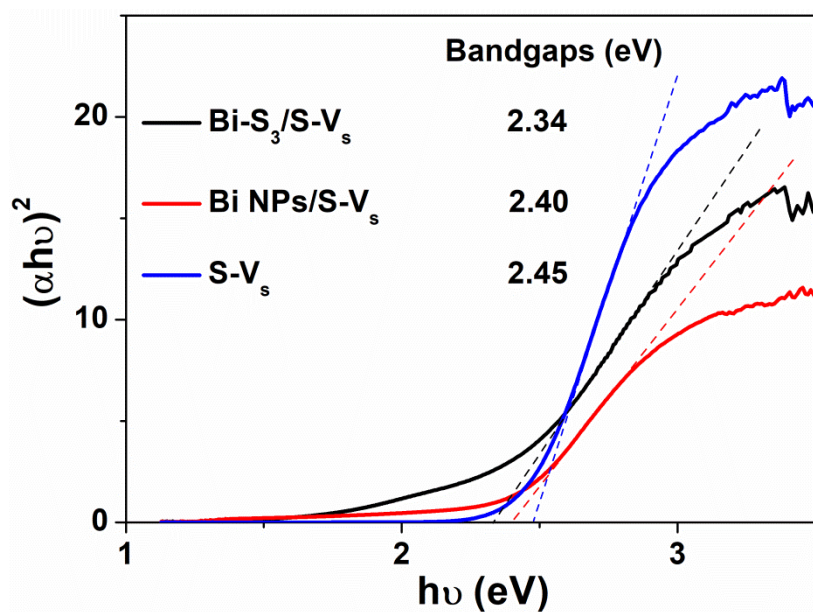


**Figure S19.**  $(\alpha h\nu)^2$  versus  $(h\nu)$  plots to calculate the bandgaps of samples.

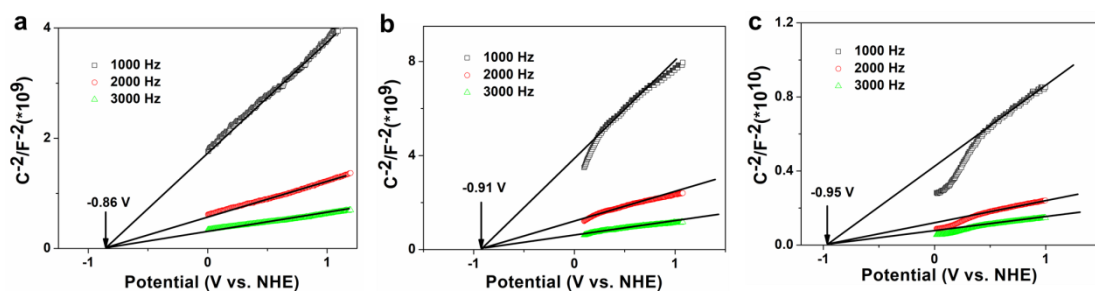


**Figure S20.** Mott-Schottky plots of different samples (a) Bi-S<sub>3</sub>/S-V<sub>s</sub>, (b) Bi NPs/S-V<sub>s</sub> and (c) S-V<sub>s</sub>.



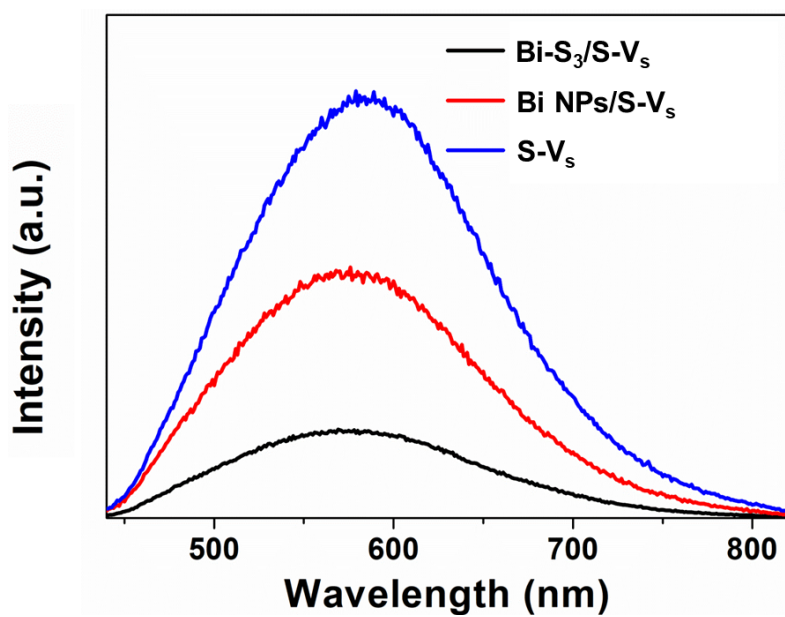


**Figure S21.** PL emission response of samples.

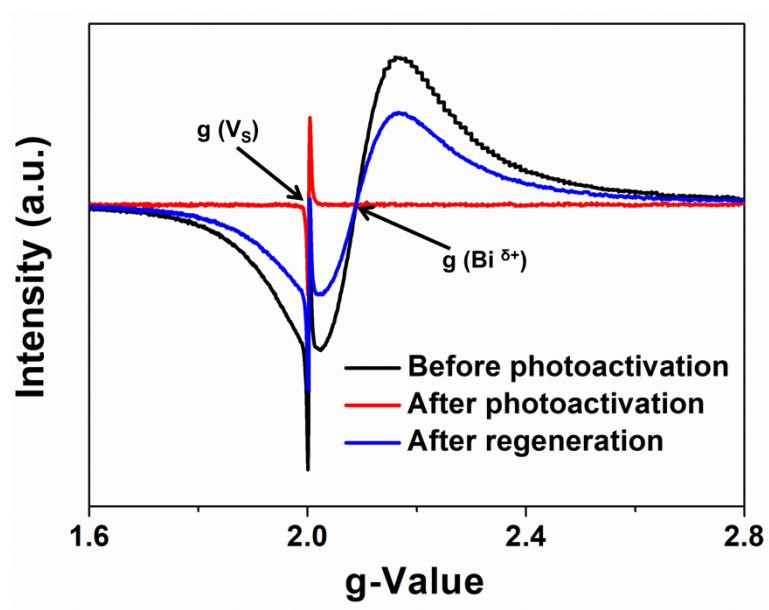


**Figure S22.** g value of Bi-S<sub>3</sub>/S-V<sub>s</sub> in various states.

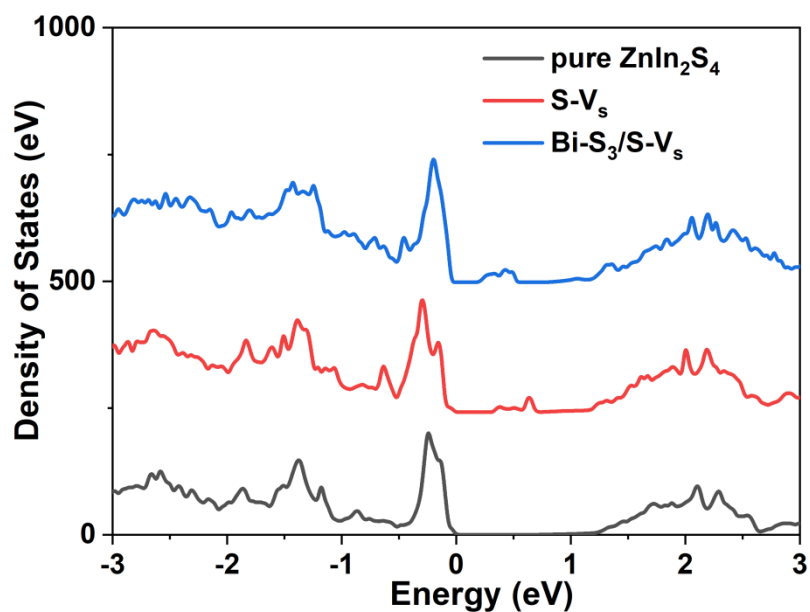


**Figure S23.** The calculated total density of states (TDOS) of pure  $\text{ZnIn}_2\text{S}_4$ ,  $\text{Bi-S}_3/\text{S-V}_s$  and  $\text{S-V}_s$ .

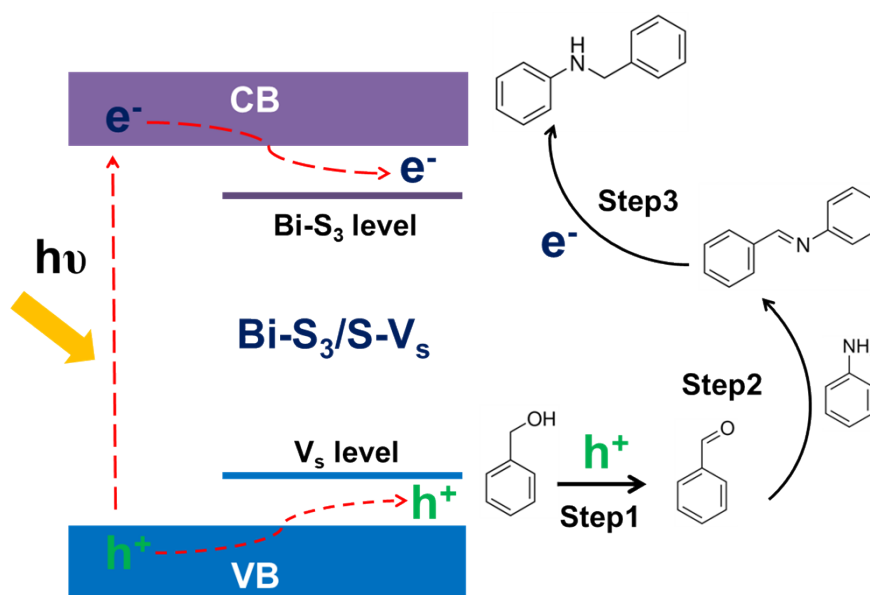
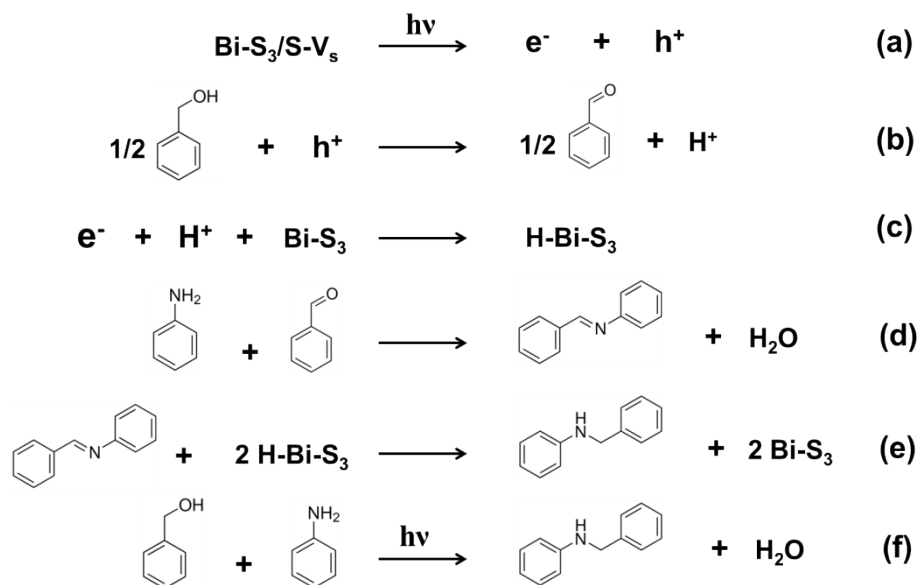


**Figure S24.** Schematic illustration of the cascade synthesis for the N-alkylation of amines by alcohols over  $\text{Bi-S}_3/\text{S-V}_s$ .



**Scheme S1.** Proposed reaction steps over Bi-S<sub>3</sub>/S-V<sub>s</sub> photocatalyst.

**Table S1.** XPS binding energies of Bi 4f and S 2p.

Sample	Bi 4f <sub>7/2</sub> (eV)	Bi 4f <sub>5/2</sub> (eV)	S 2p <sub>3/2</sub> (eV)	S 2p <sub>1/2</sub> (eV)
Bi-S <sub>3</sub> /S-V <sub>s</sub>	158.9	164.1	161.6	162.8
Bi NPs/S-V <sub>s</sub>	156.7	162.4	161.6	162.8
<i>Quasi in-situ</i> XPS Bi-S <sub>3</sub> /S-V <sub>s</sub>	158.5	163.8	161.9	163.1

XPS of Bi-S<sub>3</sub>/S-V<sub>s</sub> and Bi NPs/S-V<sub>s</sub> are displayed in Figure 2b,c and Table S1. As for the Bi-S<sub>3</sub>/S-V<sub>s</sub> samples, the binding energies of Bi 4f<sub>7/2</sub> and Bi 4f<sub>5/2</sub> were located at 158.9 eV and 164.1 eV, respectively, which were the characteristic peaks of Bi-S coordination structure.<sup>9</sup> For Bi NPs/S-V<sub>s</sub>, the binding energies of Bi 4f<sub>7/2</sub> and Bi 4f<sub>5/2</sub> were around 156.7 eV and 162.4 eV, which were assigned to Bi<sup>0</sup>.

**Table S2.** Structural parameters extracted from the Bi L3-edge space spectra fitting of Bi-S<sub>3</sub>/S-V<sub>s</sub>.

Bi-S <sub>3</sub> /S-V <sub>s</sub>	Reduced Chi-square ( $\chi^2$ )	R-factor (%)	amp/ S <sub>0</sub> <sup>2</sup>	N <sub>(Bi-S path)</sub>	R <sub>(Bi-S path)</sub> (Å)	$\sigma^2_{(Bi-S path)}$ (10 <sup>-3</sup> Å <sup>2</sup> )	$\Delta E_0$ (eV)
	125.63	0.0388	1.03+ /-0.11	3	2.531 ±0.030	2.2+/-0.6	- 4.67+/- 2.56

**Table S3.** The control experiments under different conditions.

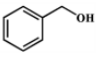
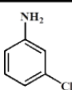
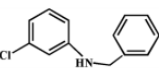
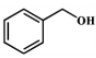
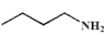
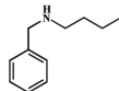
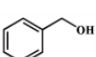
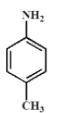
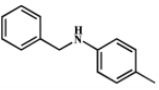
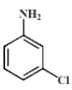
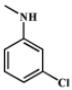
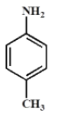
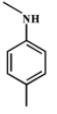
Entry	Photocatalyst	Light	Con. %	Sel. %
1	Bi-S <sub>3</sub> /S-V <sub>s</sub>	Blue LED	95.5 %	98.9 %
2	No photocatalyst	Blue LED	-- <sup>a</sup>	-- <sup>a</sup>
3	Bi-S <sub>3</sub> /S-V <sub>s</sub>	Dark	-- <sup>a</sup>	-- <sup>a</sup>

Reaction conditions: alcohols (0.5 mL), amines (0.05 mL), Bi-S<sub>3</sub>/S-V<sub>s</sub> photocatalyst (10.0 mg), 50 mg t-BuOK, room temperature, blue LED light ( $\lambda$  = 455 nm), reaction time: 12 h, atmospheric Ar. <sup>a</sup>refers to no products or negligible products detected.

**Table S4.** The selectivity of each product over samples.

Sample	N-benzylaniline Yield	N-benzylaniline Selectivity	N-benzylideneaniline Selectivity
Bi-S <sub>3</sub> /S-V <sub>s</sub>	94.5%	98.9%	<1%
Bi NPs/S-V <sub>s</sub>	35.7%	98.5%	<1%
S-V <sub>s</sub>	8.5%	98.7%	<1%
ZIS	4.1%	>99%	<1%

**Table S5.** Alcohols-based N-Alkylation of amines over Bi-S<sub>3</sub>/S-V<sub>s</sub> under blue LED light irradiation.

$  \begin{array}{c}  \text{R}_1\text{---CH}_2\text{---OH} + \text{R}_2\text{---CH}_2\text{---NH}_2 \xrightarrow[\text{LED } \lambda = 455 \text{ nm}]{\text{Bi-S}_3/\text{S-V}_s} \text{R}_1\text{---CH}_2\text{---NH---R}_2 + \text{H}_2\text{O} \\  \text{1a} \qquad \qquad \qquad \text{2a} \qquad \qquad \qquad \text{3a}  \end{array}  $						
Entry	Alcohols	Amines	Products	2a Con. %	3a Sel. %	3a Yield %
1				100%	100%	100%
2				100%	89.84%	89.84%
3				63.48%	90.31%	57.33%
4	CH <sub>3</sub> OH			66.49%	100%	66.49%
5	CH <sub>3</sub> OH			57.70%	100%	57.70%

Reaction conditions: alcohols (0.5 mL), amines (0.05 mL), Bi-S<sub>3</sub>/S-V<sub>s</sub> photocatalyst (10.0 mg), 50 mg t-BuOK, room temperature, blue LED light (λ = 455 nm), reaction time: 12 h, atmospheric Ar.

**Table S6.** Fluorescence lifetime and average lifetime results for different samples ( $\lambda_{\text{exc}}$  = 420 nm).

Sample	Bi-S <sub>3</sub> /S-V <sub>s</sub>	Bi NPs/S-V <sub>s</sub>	S-V <sub>s</sub>
$\tau_1$ (ns)	1.15	1.02	1.14
A <sub>1</sub>	505.97	494.863	536.571
$\tau_2$ (ns)	16.73	13.05	13.33
A <sub>2</sub>	87.387	54.267	50.131
$\tau_{\text{avg}}$ (ns)	12.29	8.04	7.50

## Supporting References

1. Ávila-Bolívar, B.; García-Cruz, L.; Montiel, V.; Solla-Gullón, J. Electrochemical Reduction of CO<sub>2</sub> to Formate on Easily Prepared Carbon-Supported Bi Nanoparticles. *Molecules* **2019**, *24*, 2032.
2. Zhang, Z.; Liu, K.; Feng, Z.; Bao, Y.; Dong, B. Hierarchical Sheet-on-Sheet ZnIn<sub>2</sub>S<sub>4</sub>/g-C<sub>3</sub>N<sub>4</sub> Heterostructure with Highly Efficient Photocatalytic H<sub>2</sub> production Based on Photoinduced Interfacial Charge Transfer. *Sci. Rep.* **2016**, *6*, 19221.
3. Kresse, G.; Furthmüller, J. Efficiency of Ab-initio Total Energy Calculations for Metals and Semiconductors Using a Plane-Wave Basis Set. *Comp. Mat. Sc.* **1996**, *6*, 15–50.
4. Perdew, J.; Burke, K.; Ernzerhof, M. Generalized Gradient Approximation Made Simple. *Phys. Rev. Lett.* **1996**, *77*, 3865–3868.
5. Blöchl, P. Projector Augmented-Wave Method. *Phys. Rev. B* **1994**, *50*, 17953–

- 17979.
6. Monkhorst, H.; Pack, J. Special Points for Brillouin-Zone Integrations. *Phys. Rev. B* **1976**, *13*, 5188–5192.
  7. Grimme, S.; Antony, J.; Ehrlich, S.; Krieg, H. A consistent and accurate ab initio parametrization of density functional dispersion correction (DFT-D) for the 94 elements H-Pu. *J. Chem. Phys.* **2010**, *132*, 154104.
  8. Zhang, Y., Tang, H., Gao, S. Density Functional Theory Study of ZnIn<sub>2</sub>S<sub>4</sub> and CdIn<sub>2</sub>S<sub>4</sub> Polymorphs Using Full-Potential Linearized Augmented Plane Wave Method and Modified Becke–Johnson Potential. *Phys. Status. Solidi. B* **2020**, *257*, 1900485.
  9. Lin, Y.; Yang, L.; Jiang, H.; Zhang, Y.; Bo, Y.; Liu, P.; Chen, S.; Xiang, B.; Li, G.; Jiang, J.; Xiong, Y.; Song, L. Sulfur Atomically Doped Bismuth Nanobelt Driven by Electrochemical Self-Reconstruction for Boosted Electrocatalysis. *J. Phys. Chem. Lett.* **2020**, *11*, 1746–1752.